

dominate the motion of the star for large molecular weights of the star.

**Note Added in Proof.** An  $f$ -armed star must bring  $f - 2$  arms to the branching point for a diffusive step. But the arm ends need not arrive at the branching point simultaneously so we might expect  $D$  to have a weaker  $f$  dependence than suggested in the text.

**Acknowledgment.** We thank Dr. J. Klein for useful discussions, especially as regards the diffusive mechanisms available to the entangled star. R.J.N. acknowledges the assistance of an SERC CASE award with ICI, Welwyn Garden City, U.K.

### References and Notes

(1) Evans, K. E.; Edwards, S. F. *J. Chem. Soc., Faraday Trans. 2*, 1981, 77, 1891.

- (2) Edwards, S. F.; Evans, K. E. *J. Chem. Soc., Faraday Trans. 2*, 1981, 77, 1913.  
 (3) Evans, K. E.; Edwards, S. F. *J. Chem. Soc., Faraday Trans. 2*, 1981, 77, 1929.  
 (4) de Gennes, P. G. *J. Chem. Phys.* 1971, 55, 572.  
 (5) Evans, K. E. *J. Chem. Soc., Faraday Trans. 2*, 1981, 77, 2385.  
 (6) de Gennes, P. G. *J. Phys. (Paris)* 1975, 36, 1199.  
 (7) de Gennes, P. G. "Scaling Concepts in Polymer Physics"; Cornell University Press: Ithaca, NY, 1979.  
 (8) Doi, M.; Kuzuu, N. Y. *J. Polym. Sci., Polym. Lett. Ed.* 1980, 18, 775.  
 (9) Graessley, W. W.; Roovers, J. *Macromolecules* 1979, 12, 959.  
 (10) Rouse, P. E. *J. Chem. Phys.* 1953, 21, 1272.  
 (11) Warner, M. *J. Phys. C, Solid State Phys.* 1981, 14, 4985.  
 (12) Klein, J. *Macromolecules* 1978, 11, 852.  
 (13) Daoud, M.; de Gennes, P. G. *J. Polym. Sci.* 1979, 17, 1971.  
 (14) Another calculation of  $P(N)$  differing from eq 4 only in the preexponential factor has been reported: Helfand, E.; Pearson, D. S., to be published.

## Anisotropic Molecular Motion of Spin-Labeled Poly(methyl methacrylate) Detected by ESR

M. Shiotani and J. Sohma\*

Faculty of Engineering, Hokkaido University, Sapporo 060, Japan

J. H. Freed

Department of Chemistry, Cornell University, Ithaca, New York 14853.

Received February 1, 1983

**ABSTRACT:** Anisotropic rotational motion of the side chain in poly(methyl methacrylate) (PMMA) is inferred from the detailed analysis of the ESR spectrum of spin-labeled PMMA. Rotation about the axis parallel to the N-O bond of the nitroxide label bonded at the end of the ester side chains was twice as fast as that about the axes perpendicular to this bond in the incipient motional narrowing region. This axially symmetric rotation is discussed in terms of the molecular motions of PMMA.

### I. Introduction

It has been well established that both spin-probe and spin-label techniques are very useful to characterize molecular motions in synthetic polymers<sup>1</sup> as well as biopolymers.<sup>2</sup> ESR studies of molecular motion of spin-labeled polymers have two advantages: (1) easy detection of rapid motion on the time scale of nanoseconds to picoseconds and (2) selective detection of particular molecular motion of a part of the polymer, such as the end of a side chain that is labeled by a stable paramagnetic free radical. Poly(methyl methacrylate) (PMMA) is one of the polymers on which molecular motions have been studied by ESR combined with either the spin-labeling or the spin-probe method. For example, Miller and Veksli<sup>3,4</sup> reported ESR studies of spin-labeled PMMA, and Bullock and Cameron<sup>5</sup> and Shiotani and Sohma<sup>6,7</sup> also investigated the molecular motions of PMMA by ESR. These authors<sup>3-7</sup> have analyzed the observed spectra based on the assumption that the rotational reorientation was isotropic. Evaluation of the correlation time,  $\tau_R$ , of the rotational motion involved in spin-labeled PMMA relied upon the simplified expression of  $\tau_R$  proposed by Freed et al.<sup>8-11</sup> for isotropic rotation in the slow-motional region ( $10^{-9}$  s  $\leq$   $\tau_R$   $\leq$   $10^{-6}$  s) and Kivelson's expression<sup>12</sup> for isotropic rotation in the motional narrowing region ( $10^{-11}$  s  $\leq$   $\tau_R$   $\leq$   $10^{-9}$  s).

In previous studies,<sup>6,7</sup> the present authors also used these expressions as well as other simple expressions<sup>7,13</sup> for partial averaging to analyze the spectra. However, later investigation has shown that such an assumption is too simplified. There is no good reason to assume isotropic

motion for a labeling radical at the end of the ester chain of PMMA. It is more reasonable to allow for anisotropy in this particular molecular motion. In fact, Pilař et al.<sup>14a</sup> observed ESR spectra of the spin labels attached to the side chain of poly(methacrylamide)-type copolymers and concluded that the rotational reorientation was quite anisotropic and depended on the type of side chain. Freed and his collaborators<sup>11</sup> have developed an extensive theory of ESR spectra of nitroxides, which allows one to calculate the line shape for ESR spectra with a broad range of correlation times ( $10^{-12}$  s  $\leq$   $\tau_R$   $\leq$   $10^{-6}$  s) and to treat various models of anisotropic rotational reorientation.

In this paper we report results obtained for spin-labeled PMMA with an analysis carried out in terms of the theory of Freed et al., and we compare these results with our earlier ones.

### II. Experimental Section

PMMA, which was spin labeled by a nitroxide radical at the end of the ester side chain, is the same sample used for the previous experiments.<sup>6,7</sup> One out of every 100 side chains was labeled by the nitroxide radicals. The details of the preparation of the polymer are described in the previous papers. A JEOL PE-X spectrometer was used with 100-kHz modulation, and the temperature control unit was used for temperature variation experiments.

### III. Analysis of ESR Line Shape

Temperature variations of the ESR spectra of the spin-labeled PMMA are shown in Figure 1. No change in the line shape was found at temperatures below 9 °C.

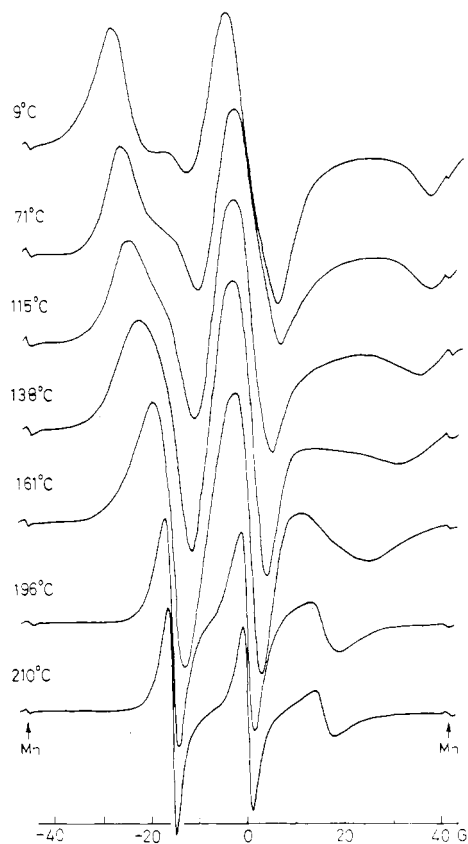


Figure 1. Temperature-dependent ESR spectra of spin-labeled PMMA.

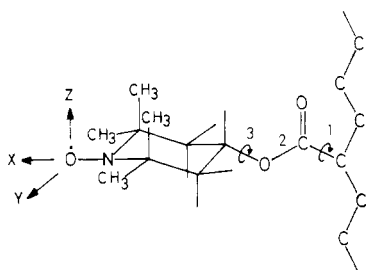


Figure 2. Structure of spin-labeled PMMA with 2,2,6,6-tetramethyl-4-hydroxypiperidinyl-1-oxyl and the assumed conformation of spin label bounded at the end of the side chain.

ESR parameters  $\bar{g}$  and  $\bar{A}$  were determined as the values that gave the best fitting simulation to the spectrum observed in the frozen state at temperature below 9°C. They are  $g_X = 2.0092$ ,  $g_Y = 2.0062$ ,  $g_Z = 2.0022$ ,  $A_X = 7.6$  G,  $A_Y = 6.4$  G,  $A_Z = 32.8$  G, and 4.0 G for the line width  $1/T_2$ . The subscripts X, Y, and Z represent the principal axes of these tensors, as shown in Figure 2 with reference to the molecular structure.

(1) **Isotropic Molecular Motion.** The spectral simulations were carried out based on a Brownian motional model<sup>11</sup> for isotropic rotational diffusion. The best simulated spectra are shown with dotted lines in Figure 3. The simulations of these spectra represent the main features of the observed spectra at various temperatures, but the agreement between the simulated and the observed spectra at each temperature is not entirely satisfactory. Especially in the higher temperature region, i.e., incipient motional narrowing region, a qualitative difference was found in the relative intensities of the triplet; the central peak appears the highest in the theoretical spectrum based on the isotropic molecular motion, while the peak at the lower field is the highest in the observed spectrum (Figure

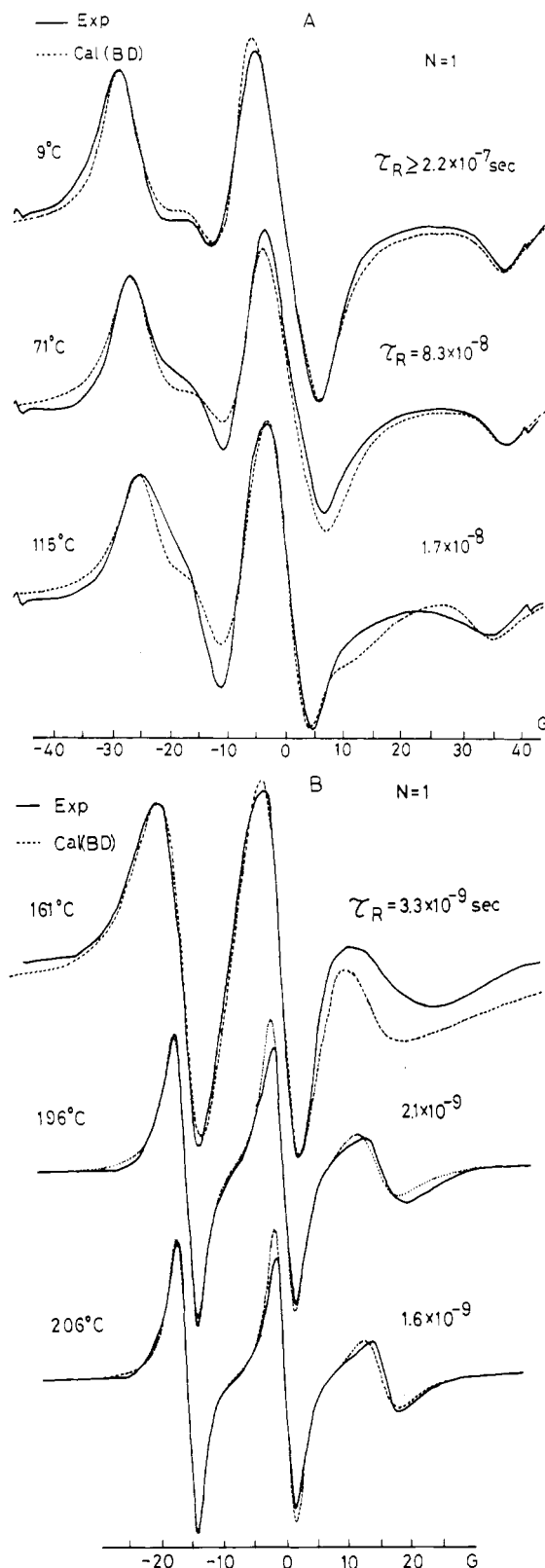
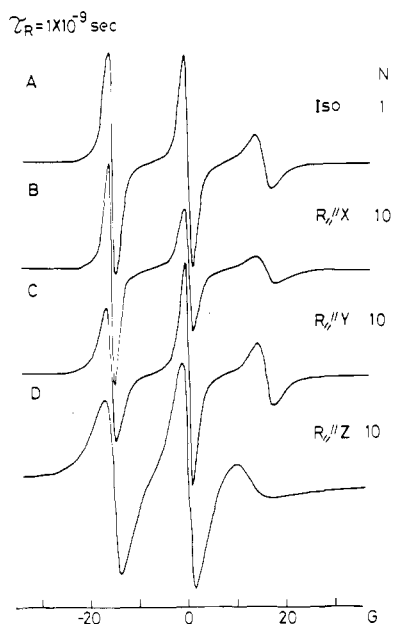


Figure 3. Line shape of experimental spectra compared with that of calculated spectra using an isotropic Brownian diffusion model.

3B). This disagreement clearly suggests that the molecular motion of the labeling molecule at the end of the ester side chain in PMMA is not isotropic.

(2) **Axially Symmetric Rotation.** Anisotropic rotation is described by a rotational diffusion tensor, the principal values of which are written as  $R_X$ ,  $R_Y$ , and  $R_Z$ . More simply, the rotational reorientation of nitroxides is characterized by an axially symmetric rotational diffusion



**Figure 4.** Theoretical spectra of anisotropic rotation about its  $Z$  axis (B),  $Y$  axis (C), and  $Z$  axis (D). The spectra were calculated for the Brownian rotational diffusion model using  $R_{\parallel} = 5.3 \times 10^8 \text{ s}^{-1}$ ,  $R_{\perp} = 5.3 \times 10^7 \text{ s}^{-1}$  (i.e.,  $N = R_{\parallel}/R_{\perp} = 10$ ;  $\tau_R = [6(R_{\parallel}R_{\perp})^{1/2}]^{-1} = 1 \times 10^{-9} \text{ s}$ ), and  $1/T_2^{\circ} = 0.5 \text{ G}$ . For isotropic rotation (A)  $R_{\parallel} = R_{\perp} \approx 1.67 \times 10^8 \text{ s}^{-1}$  was used.

tensor,  $R_X = R_Y = R_{\perp}$  and  $R_Z = R_{\parallel}$ . The degree of anisotropy of the rotational reorientation is expressed by the relation  $N = R_{\parallel}/R_{\perp}$ . It is assumed in the first approximation that the symmetry axis of the rotational diffusion tensor,  $Z'$ , is identical with one of the molecular axes of the nitroxide molecule (Figure 2). Theoretical spectra were calculated with a Brownian rotational diffusion model<sup>11</sup> in order to demonstrate how the line shape varies when the molecular axis about which rapid rotation takes place is changed from the  $Z$  to the  $X$  or  $Y$  axis (Figure 2). For the calculation the degree of anisotropy was assumed to be  $N = 10$  with a constant correlation time of  $\tau_R = 1 \times 10^{-9} \text{ s}$  (mean correlation time for anisotropic rotation being defined by  $\tau_R = [6(R_{\parallel}R_{\perp})^{1/2}]^{-1}$  for Brownian rotational diffusion).<sup>11</sup> When the symmetry axis is parallel to the  $X$  axis of the molecular coordinates, the theoretical spectrum derived from Freed's theory appears as pattern B in Figure 4. Similarly, when the symmetry axis is taken parallel to either the  $Y$  or the  $Z$  axis, the theoretical spectrum is either pattern C or pattern D, respectively. The important characteristic of the observed spectrum is the highest peak occurring at the low-field side in the triplet. This characteristic appears only in pattern B among the four theoretical line shapes shown in Figure 4. Therefore, it is reasonable to conclude that the rotational symmetry axis is parallel (or almost parallel) to the  $X$  axis of the molecular coordinates. Before searching for the best fit pattern by varying  $\tau_R$  and  $N$ , we want to show how sensitively the ESR line shape varies with the value of  $N$ , which is the parameter expressing anisotropy in the rotational diffusion. The theoretical spectra shown in Figure 5 were calculated for Brownian diffusion with the  $Y$  axis as the symmetry axis using a typical value of  $\tau_R = 1 \times 10^{-9} \text{ s}$  (i.e., the incipient motional narrowing region),  $N$  being varied from 1 to 10. By comparison of the line shape observed at  $210^{\circ} \text{C}$  with the theoretical patterns, one may find that the line shape derived from  $N = 2$  is close to the observed spectrum. Further analysis was tried to obtain more accurate values of  $\tau_R$  and  $N$  from the spectrum observed at each temperature, especially in the incipient

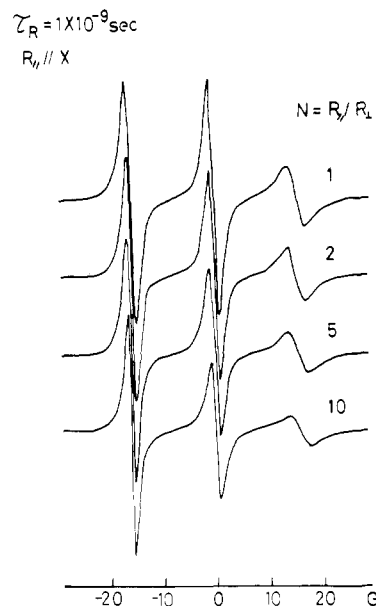


**Figure 5.** Theoretical spectra of anisotropic rotation about its  $X$  axis illustrating the change in the line shape as a function of degree of anisotropy,  $N$ . The spectra were calculated for the Brownian diffusion model using a constant rotational correlation time,  $\tau_R = 1 \times 10^{-9} \text{ s}$ , and  $1/T_2^{\circ} = 0.5 \text{ G}$ .

motional narrowing region. By incipient motional narrowing we mean  $\tau_R \geq 10^{-9} \text{ s}$ , where slow-motional effects may be present but should not be large. ESR spectra of nitroxides in the motional narrowing region consist of a triplet due to the  $^{14}\text{N}$  hyperfine splitting with different line widths and consequently with different amplitudes. The intrinsic peak-to-peak derivative line width,  $1/T_2$ , of triplet may be fitted to the expression<sup>9,11</sup>

$$1/T_2(M_I) = A + BM_I + CM_I^2$$

where  $M_I$  is the spectrum index number;  $M_I = +1, 0$ , and  $-1$  for low-field, central, and high-field lines, respectively. Using the inverse proportionality of the line widths to the square root of their first-derivative peak-to-peak heights, one can determine the relative magnitudes of  $A$ ,  $B$ , and  $C$  to a higher accuracy from the measured peak-to-peak heights. Then the line width of one of the peaks, usually the central line, is used for absolute magnitudes. In the present studies, we determined the ratios  $B/A$  and  $C/A$  from the peak-to-peak heights. The determination of the absolute widths (including effects of inhomogeneous broadening) was obtained in the detailed spectral simulations as described below. The theoretical values of  $B/A$  and  $C/A$  were determined from theoretical spectra calculated for a Brownian rotational diffusion model in the incipient motional narrowing region as a function of the correlation time  $\tau_R$ , degree of anisotropy  $N$ , and symmetry axis of the rotational diffusion tensor  $\hat{R}$  characterizing the rotational reorientation. (These calculations include any slow-motional effects.) It should be noted that (1) the contribution of unresolved hyperfine splitting to the line width was simply introduced at this stage in the analysis as an additive contribution to the  $A$  term, (2) small corrections for incipient slow motion (i.e.,  $\tau_R > 1 \times 10^{-9} \text{ s}$ ) are automatically introduced, and (3) the ESR spectra are independent of model in the region of (incipient) motional narrowing.<sup>9,11</sup> The theoretical values of  $C/A$  and  $B/A$  determined for anisotropic rotation along the  $X$  axis are plotted as a function of  $\tau_R$  and  $N$  in Figure 6. By comparing the experimentally determined  $C/A$  vs.  $B/A$  temperature dependence, it is possible to determine the  $N$  and the respective correlation time as shown in the figure. The

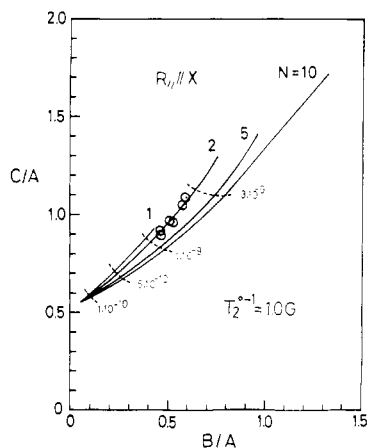


Figure 6. Comparison of experimental ( $\odot$ ) and calculated (—)  $C/A$  vs.  $B/A$  dependence.

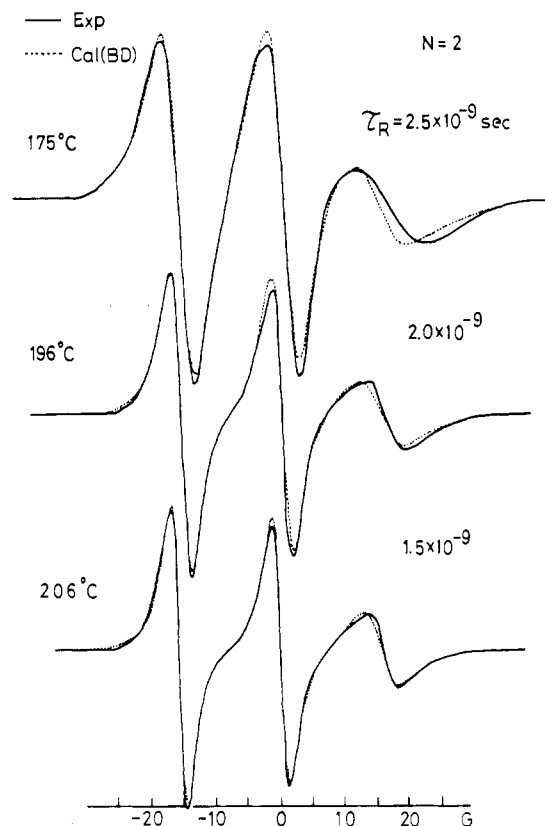


Figure 7. Motional narrowing experimental spectra compared with the best fit theoretical ones. The intrinsic line width of  $1/T_2^\circ$  used in the calculation was 2.0 G for the upper spectrum, but 1.0 G for the middle and lower spectra.

experimental data appear to be fitted well by the curve for  $N = 2$ .

To confirm the validity of this analysis the theoretical spectra were then simulated by using the best fit values from the  $C/A$  vs.  $B/A$  relation and compared with experimental ones at each temperature in Figure 7. The good agreements between the experimental and calculated spectra convince us that the simple analysis using the ratios  $C/A$  and  $B/A$  with small incipient slow-motional corrections and simple introduction of effects of inhomogeneous broadening leads to rather good estimates of the correlation time and the degree of anisotropy. Furthermore, by comparing the case of anisotropic rotation ( $N = 2$  in Figure 7) with that of the isotropic one ( $N = 1$  in Figure 3B), it is clearly seen that the fit is much improved by introducing anisotropy in the rotational reorientation.

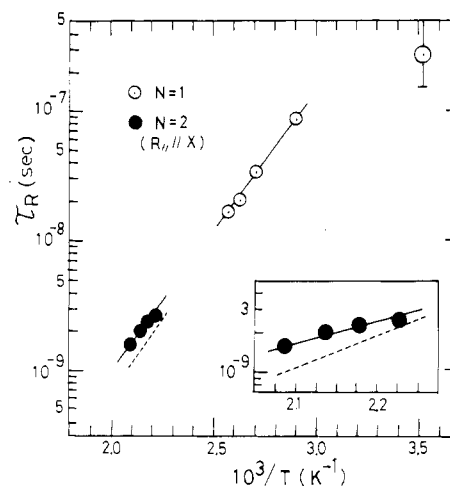


Figure 8. Plots of  $\tau_R$  (s) vs.  $1/T$  ( $K^{-1}$ ).

Arrhenius plots of  $\tau_R$ 's are shown in Figure 8, in which filled circles are the data determined from the spectra shown in Figure 7 ( $N = 2$ ) and open circles are those obtained from the patterns in Figure 3B ( $N = 1$ ). The dotted curve is an Arrhenius plot of the correlation times derived from the isotropic rotation.<sup>7</sup> The activation energy was estimated as 9.3 kcal/mol for the  $\tau_R$  derived from the anisotropic rotation, while the activation energy in the same temperature region was 9.7 kcal/mol derived from the isotropic rotation in the former paper.<sup>7</sup> Thus, no marked differences were found in both the correlation time and the activation energy once anisotropy is introduced in the analysis of the spectra. This fact plus the small value of  $N$  seems to suggest that isotropic rotation is a good first approximation for the molecular motion at the ends of ester side chains in PMMA at these temperatures. The  $\tau_R$ 's in the temperature region below  $T_g$  are also on a straight line, which gives an activation energy similar to either one of the values mentioned above. It is hard to determine that these  $\tau_R$ 's are on an extension of either one of the Arrhenius plots in the higher temperature region, taking account of errors involved in both the measurements and the extension. Moreover, another model, a jump-type model,<sup>11</sup> might fit the experiments better than the Brownian model assumed in this analysis. On this point further analysis is in progress, and we omit the discussion on  $\tau_R$ 's in the lower temperature region in this paper.

However, it should be stressed that the analyses of the observed ESR spectra based on the Freed theory provide us with interesting information on the anisotropy in the molecular motion in PMMA, which is hardly detected by experimental techniques other than ESR. Thus, the quantitative detection of anisotropy in molecular motions of labeling molecules in the incipient motional narrowing region is an important feature of ESR studies of molecular motions.

#### IV. Discussion

Molecular motions detected by ESR are at the sites that are labeled by nitroxides. There are many degrees of freedom for rotations in polymeric systems, and therefore the rotational motion of the nitroxides at the ends of the ester side chains of PMMA molecules is a superposition of the various rotational motions at the temperature of observation. In such a case, the rotational diffusion tensor determined by our ESR study is really a composite. This composite or effective  $\mathbf{R}$  tensor may be related to the various internal and overall modes of motion along lines

previously suggested by Freed and co-workers.<sup>14b</sup> In that work, a number of special cases leading to simplified interpretations of this effective  $\mathbf{R}$  tensor are pointed out. Although there exist many internal rotational modes in a polymeric molecule because of the many degrees of freedom for rotation about each C–C bond, the main modes of rotation are the following three: (i) rotation of the molecule as a whole, (ii) micro-Brownian motion of the C–C bonds in the main chain, and (iii) rotations of the side chains. Although overall rotational motion of the molecules is possible even in the solid phase, it is hard to imagine that the rate of the rotation is as high as of the order of a nanosecond as determined by our experiments; the Einstein–Stokes law indicates that the rotational rate of a bulky molecule such as a polymer is very small in a viscous matrix like solid PMMA. Thus, it is reasonable to neglect the contribution of the overall rotation of the molecule to the observed rate of the rotation. The second possible mode of rotation consists of the rotations of the C–C bonds in the PMMA main chains. The anisotropy in motion was inferred from a comparison of the theoretical line shapes with those observed in the temperature range 160–210 °C. The glass transition of PMMA occurs at about 110 °C.<sup>15</sup> Micro-Brownian motion of the PMMA main chain is very active in this temperature range, and the rate of the rotation could be as high as  $10^9 \text{ s}^{-1}$ . However, micro-Brownian motion of polymer molecules is isotropic,<sup>16</sup> and the rotation resulting from the micro-Brownian motion should be isotropic. This is not what we observe: the detected rotation is anisotropic. Thus, it is quite possible that the micro-Brownian motion of the main chain is not the detected rotational motion, although motion of the main chain may provide a background contribution. The last mode of rotation, i.e., rotations of the ester side chains, is believed to be the dominant motion detected in our experiments. The activation energy for rotation, 9.3 kcal/mol, determined by this experiment is smaller than that for micro-Brownian motion (40–150 kcal/mol)<sup>17</sup> but closer to that typically observed for side-chain motion (ca. 19 kcal/mol).<sup>18,19</sup> This smaller value of the activation energy supports our belief that the primary detected motion is the rotational motion of the ester side chains. There are three possible rotational modes in a side chain: rotations about bond 1, bond 2, or bond 3 (cf. Figure 2). The conclusion derived from the analysis of the experimental results is that the faster rotation is about an axis parallel to the N–O bond in the nitroxide and the slower rotation about the axes perpendicular to the N–O bond. Rotation about bond 2 is more hindered than those about the other two axes because of the partial double-bond nature. Thus one may rule out this rotation. Rotation about bond 1 should require more activation energy than that about bond 3, because more free volume is re-

quired for rotation about bond 1. Actually 19 kcal/mol is estimated as the activation energy for the rotation of the ester side chain as a whole.<sup>18–20</sup> The smaller value, 9.3 kcal/mol, for the observed activation energy suggests that the dominant rotation detected by ESR is a part of the ester side chain. Therefore, it is reasonable to assume that the observed changes of the ESR line shape in the temperature range 160–200 °C is mainly affected by rapid rotation about bond 3 in the ester side chains, yet we must invoke some coupling to the other modes of motion in order to explain the rather small motional anisotropy ( $N = 2$ ). It appears, therefore, that the molecular motion detected by the ESR of spin-labeled PMMA is the rotational motion of the labeling molecule at the end of the ester side chains, but which is modified by other modes of the polymer.

**Acknowledgment.** Part of this work was performed at the Department of Chemistry, Cornell University, where M.S. spent a leave of absence. This work was supported by NSF Grant No. CHE 8024124 and NIH Grant No. GM25862.

**Registry No.** Poly(methyl methacrylate), 9011-14-7.

## References and Notes

- Boyer, R. F.; Keinath, S. E., Ed. "Molecular Motion in Polymers by ESR"; Harwood Academic Press: New York, 1978; MMI Press Symposium Series, Vol. 1.
- Berliner, L. J., Ed. "Spin Labeling. I. Theory and Application"; Academic Press: New York, 1976.
- Miller, W. G.; Vekslis, Z. *Rubber Chem. Technol.* **1975**, *48*, 248.
- Vekslis, Z.; Miller, W. G. *Macromolecules* **1975**, *8*, 248.
- Bullock, A. T.; Cameron, G. C.; Krajewski, V. *J. Phys. Chem.* **1976**, *80*, 1972.
- Shiotani, M.; Sohma, J. *Rep. Prog. Polym. Phys. Jpn.* **1974**, *17*, 505.
- Shiotani, M.; Sohma, J. *Polym. J.* **1977**, *9*, 283.
- Goldman, S. A.; Bruno, G. V.; Freed, J. H. *J. Phys. Chem.* **1972**, *76*, 1858.
- Goldman, S. A.; Bruno, G. V.; Polnaszek, C. F.; Freed, J. H. *J. Chem. Phys.* **1972**, *56*, 716.
- Mason, R. P.; Freed, J. H. *J. Phys. Chem.* **1974**, *78*, 1321.
- Freed, J. H., Chapter 3 in ref 2.
- Kivelson, D. *J. Chem. Phys.* **1960**, *33*, 1904.
- Moriuchi, S.; Sohma, J. *Mem. Fac. Eng., Hokkaido Univ.* **1974**, *13*, 335.
- (a) Pilař, J.; Labský, J.; Kálal, J.; Freed, J. H. *J. Phys. Chem.* **1979**, *83*, 1907. (b) Campbell, R. F.; Meirovitch, E.; Freed, J. H. *Ibid.* **1979**, *83*, 525.
- Sinnotto, K. M. *J. Polym. Sci., Part C* **1966**, *14*, 141.
- Beuche, F. "Physical Properties of Polymers"; Interscience: New York, 1962.
- Johnson, F.; Randon, J. C. *J. Polym. Sci., Polym. Chem. Ed.* **1973**, *11*, 1995.
- Ishida, Y.; Yamafuji, K. *Kolloid-Z.* **1961**, *177*, 97.
- Tetsutani, T.; Kakizaki, M.; Hideshima, T. *Polym. J.* **1982**, *14*, 305.
- McCrum, N. G.; Read, B. E.; Williams, G. "Anelastic and Dielectric Effects in Polymer Solids"; New York, 1967; Chapter, 8.